HTML ABSTRACT + LINKS

Optical studies of metallodielectric photonic crystals: Bismuth and gallium infiltrated opals

V. Kamaev, V. Kozhevnikov, and Z. V. Vardeny[a)]
Physics Department, University of Utah, Salt Lake City, Utah 84112

P. B. Landon and A. A. Zakhidov
Nano Tech Institute, University of Texas at Dallas, Richardson, Texas 75083

(Received 26 September 2003; accepted 11 December 2003)

We have fabricated three-dimensional metallodielectric photonic crystals that consist of bismuth and gallium metals infiltrated into porous synthetic opals that have 300 nm diam silica balls. The specular reflectivity was measured in a broad spectral range from 0.3 to 25 μm using a variety of light sources, detectors and spectrometers. In addition to broadening of the original Bragg stop bands in the visible spectral range that give rise to iridescence colors, we also found a dramatic decrease of reflectivity in the visible/near-infrared spectral range. For frequencies below a cut-off frequency in the mid-infrared range the reflectivity increases to its normal bulk value in the respective metal, as predicted by theory and fitted by a model calculation. © *2004 American Institute of Physics.* [DOI: 10.1063/1.1645676]

I. INTRODUCTION

Recently there has been growing interest in studying three-dimensional (3D) metallodielectric photonic crystals (MDPCs) with submicron lattice constants that include fabrication methods,[1–13] measurements of physical properties,[8,10–13] and theoretical calculations.[14–20] There are two main goals underlying these efforts: (1) to obtain a complete photonic band gap in the visible/near-infrared (NIR) spectral range,[17] and (2) to obtain a ''transparent metal'' with low reflectivity in the visible/NIR spectral range[16,19,20] but, nevertheless, high electrical conductivity. These seemingly contradictory properties are not only scientifically interesting but also would initiate various opto-electronic applications. Theoretically it was predicted[17] that the Bragg stop bands of dielectric PCs in the visible spectral range would dramatically broaden in MDPCs due to the larger difference in dielectric constant between the respective metal and dielectric constituents. It was also predicted[16] that there would be a considerable redshift of the metallic plasma frequency, ω_p in 3D MDPCs, which for most metals is found in the ultraviolet (UV) spectral range, into the THz or mid-IR spectral range. This plasma frequency redshift is predicted to be below a cut-off frequency,[15] $\omega_c \approx c/2d$, where c is the speed of light and d is the lattice constant, which is due to waveguiding characteristic properties in 3D MDPC composite materials. Some of these predictions were confirmed in the microwave frequency and mid-IR ranges mainly for one-dimensional (1D) and two-dimensional (2D) periodic structures. To date, however very few experimental studies of 3D MDPCs have been conducted, that aimed at verifying these theoretical predictions in the visible/NIR spectral range.

a)Electronic mail: val@physics.utah.edu

II. EXPERIMENT

In this work we have fabricated 3D MDPCs that consist of metals infiltrated into porous synthetic opal PCs. Two different metals were chosen for opal infiltration: bismuth (Bi), which is a semimetal, and gallium (Ga) which has typical metallic properties. The specular reflectivity of the infiltrated and uninfiltrated opals, as well as that of the pure metals, was subsequently measured over a broad spectral range from 0.3 to 25 μm using several combinations of light sources, detectors and spectrometers. We found that the optical reflectivity spectra of the MDPC samples dramatically decrease in the visible/NIR spectral range, and recuperate in the mid-IR range below a cut-off frequency. In addition, some of the MDPC samples showed relatively bright iridescence colors caused by a broad Bragg stop band in the visible range[21] that is formed due to the enhanced optical penetration depth in the composites compared to the skin depth for the pure metals.

Opal PCs as templates for metal infiltration were grown by sedimentation of 300 nm diam silica balls in aqueous solution.[21] Some opals for gallium infiltration were received from OPALON, Russia. The resulting synthetic opals consisted of microcrystals with characteristic size of tens of μm and preferable vertical orientation along the (111) crystallographic direction. For gallium infiltration, liquid Ga (99.999% purity) was added to the opal sample at pressure of 10^{-6} Torr. Temperature of 1000 K and pressure of 600 bar were then applied for 3–5 min; the subsequent cooling was accompanied by slow pressure release during the solidification process.[22] The bismuth infiltration process was similar to that for Ga except that higher pressure (1–10 kbar) and longer exposure time (10 min to a few hours) were applied.[10] The resulting MDPC samples were approximately $5\times5\times1$ mm^3 with the flat surface area perpendicular to (111), suitable for the specular reflectivity measurements. The obtained MDPCs were electrically conductive and showed

 © 2004 American Institute of Physics

Downloaded 01 Dec 2009 to 155.97.11.183. Redistribution subject to AIP license or copyright; see http://jap.aip.org/jap/copyright.jsp

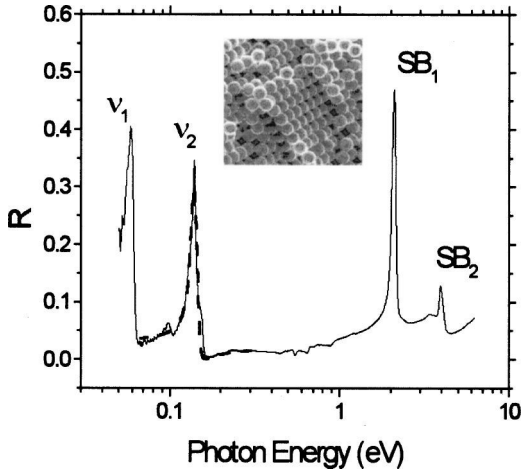

FIG. 1. The reflectiviey spectrum, $R(\omega)$, of an uninfiltrated opal PC (SEM image is shown in the inset). Various reflectivity bands are assigned: SB indicates Bragg stop bands and ν denotes silica IR active phonons. Fitting of the ν_2 band using Eq. (2) is also shown (dashed line).

network topology. We estimated the metal filling factor of the voids, f, by several techniques including measurement of the average density, and also reversing the infiltration by dissolving the metal. We found that f for Bi MDPC was $80\pm 10\%$, and f for Ga MDPC was 100%.

The specular reflectivity, $R(\omega)$, from 0.3 to 4.1 μm was measured for the MDPCs, metallic films and uninfiltrated opal samples using a homemade spectrometer that consists of various incandescent light sources (tungsten–halogen and glow-bar lamps), solid-state detectors (enhanced-UV Si, Ge and InSb), and a 0.3 met monochromator (Action Research Corporation) that was equipped with several gratings in order to span the broad spectral range. The incident light beam was directed so as to be about 13° from the surface normal. $R(\omega)$ in the mid-IR range (1.6–25 μm) was measured using a Fourier transform IR (FTIR) spectrometer (Bruker) with 4 cm^{-1} resolution. The $R(\omega)$ spectra obtained from the two spectrometers were normalized by that of silver or gold plated mirrors measured under the same conditions and also to each other at the respective overlapping spectral ranges. Since the melting temperature of Ga is $\approx 10\,^{\circ}C$ it was necessary to place the Ga MDPC sample in a cryostat at 100 K; the Bi MDPC samples, on the other hand, were measured at ambient.

Figure 1 shows a typical scanning electron micrograph (SEM) and $R(\omega)$ spectrum of the uninfiltrated opal. Four relatively sharp bands are apparent: two (SB_1 and SB_2) in the visible spectral range, and two (ν_1 and ν_2) in the mid-IR range. SB_1 at ≈ 2 eV and SB_2 at ≈ 4 eV are two Bragg stop bands (SBs) (first and second order, respectively), which are formed in the PCs due to constructive interference from silica planes along (111).[21] In contrast, ν_1 and ν_2 bands at approximately 0.06 and 0.14 eV, respectively, correspond to IR active optical phonons in silica;[23] these are the O–Si–O bond stretching and bond rocking vibrations, respectively. Otherwise $R(\omega)$ in the near- and mid-IR spectral ranges is quite low ($R\approx 1\%-3\%$).

Figure 2(a) shows the $R(\omega)$ spectrum of a 200 nm thick

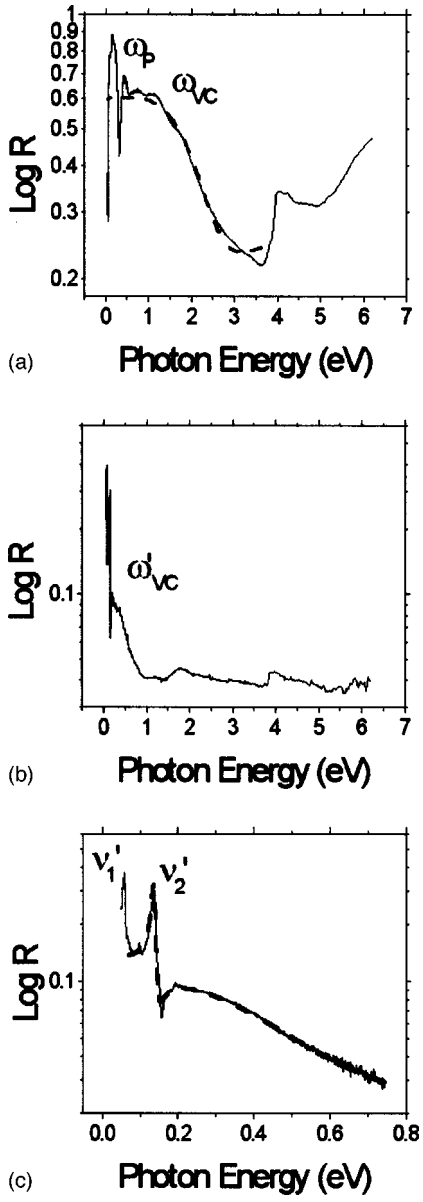

FIG. 2. $R(\omega)$ spectra of bismuth (a), and Bi-infiltrated opal (b), (c). Various bands are assigned, where ω_p is the plasma frequency, ω_{VC} is an interband transition, and ν_2' is a modified IR active phonon. The dashed lines in (a) and (c) are fits using Eqs. (1) and (3).

bismuth film deposited on a glass substrate. It is known that the semimetal bismuth has several reflective bands throughout the visible/IR spectral range that are due to allowed optical transitions from various valence subbands to corresponding conduction subbands.[24] Our measurements reveal some of them: there is a prominent shoulder at ≈ 4 eV, a broad peak at about 1.4 eV (denoted here ω_{VC}), and small peaks at ≈ 0.7 and ≈ 0.4 eV. Due to the small concentration of free carriers ($\approx 10^{18}$ cm^{-3}) the corresponding plasma frequency in bismuth was found to be in the far-IR range,[25,26] and thus is not shown in Fig. 2(a).

Figures 2(a) and 2(c) show $R(\omega)$ of the bismuth infiltrated opal. Except for the small band at about 4 eV that is related to a corresponding peak in pure Bi, and a relatively broad band at about 1.9 eV that may be related to a modified SB_1 in the uninfiltrated opal, $R(\omega)$ is almost flat in the vis-

Downloaded 01 Dec 2009 to 155.97.11.183. Redistribution subject to AIP license or copyright; see http://jap.aip.org/jap/copyright.jsp

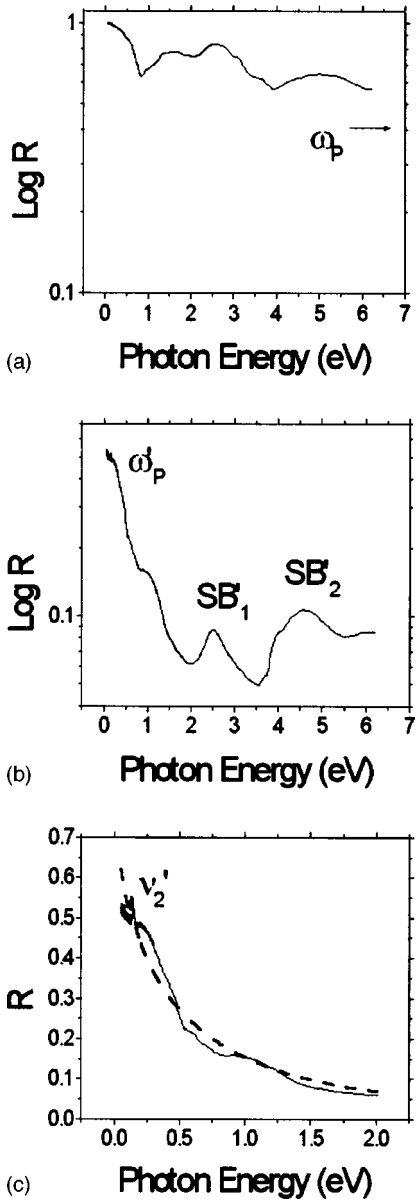

FIG. 3. Same as Fig. 2 but for gallium and Ga-infiltrated opal. SB'_1 and SB'_2 are modified stop bands.

ible and UV spectral ranges, with a value of 4% or less, $R(\omega)$ has a minimum at ≈ 1 eV, followed by a prominent increase towards lower frequencies at ω'_{VC}. We speculate that this rise in $R(\omega)$ is due to the modified ω_{VC} transition. At low frequencies there are also two reflectivity peaks in $R(\omega)$, namely, ν'_1 and ν'_2, that correspond to the modified IR active optical phonons in silica; they are seen more clearly in Fig. 2(c).

Figure 3(a) shows $R(\omega)$ of pure gallium. The free electron plasma frequency, ω_p of Ga is at about 14 eV,[27] and thus lies outside our spectral range. In the measured spectral range $R(\omega)$ is rather flat at $R \approx 70\% - 80\%$ with a moderate increase to $R \approx 100\%$ at low frequencies. Figures 3(b) and 3(c) show $R(\omega)$ of Ga-infiltrated opal. There are two well-defined stop bands in the visible and UV ranges, namely, SB'_1 at 2.5 eV and SB'_2 at 4.5 eV; these are the modified Bragg stop bands in Ga MDPC that correspond to the SB bands in the uninfiltrated opal. Otherwise $R(\omega)$ is rather small in these spectral ranges, with $R \approx 5\%$. Starting at 2 eV, however, $R(\omega)$ increases towards lower frequencies, reaching a value of about 53% in the mid-IR range [Fig. 3(c)]. We interpret this rise in $R(\omega)$ as due to the modified plasma frequency (ω'_p) that is redshifted compared to ω_p in pure Ga, as predicted by theory.[15,16] In addition, we also see a small peak ν'_2 at 0.14 eV that is related to the corresponding IR active phonon in silica.

Qualitatively, $R(\omega)$ spectra of Bi- and Ga-infiltrated opals have optical features similar to those of the corresponding pure metals and uninfiltrated opals. The MDPC samples show an increase in $R(\omega)$ at low frequencies that is typical of metallic free electron plasma, but also show stop bands in the visible spectral range that are typical of PCs. The stop bands in the MDPC samples are broader and their frequencies are blueshifted compared to those of uninfiltrated opals. Bi MDPC has a weak SB in the visible spectral range, whereas Ga MDPC has two well-defined stop bands (SB'_1, SB'_2), both of which are blueshifted approximately 0.5 eV compared to the corresponding stop bands in the opal. The shifting and broadening of the stop bands in the fabricated MDPCs may be associated with a modified refraction index in the visible spectral range, and a larger difference in refraction index between the silica and metal constituents. However, the broadening may also be due to a nonzero extinction coefficient in the infiltrated metals, which would lead to light absorption that limits the number of silica ball planes that can constructively interfere. These factors cannot be easily evaluated analytically and thus should be modeled using computer simulations. An alternative explanation for the broadening is that metal infiltrated into the opal would introduce additional disorder due to inhomogeneous filling. Also there is a rise in $R(\omega)$ at low frequencies for both MDPC samples, which leads in Bi MDPC to a redshift in ω_{VC}, and in Ga MDPC to a smaller plasma frequency that changes from $\omega_p = 14$ eV in pure Ga to $\omega'_p = 2$ eV in Ga MDPC.

III. THEORY

In order to gain insight into the optical processes that govern the dielectric function, $\varepsilon(\omega)$, of the MDPC samples we try to fit their reflectivity spectra in the infrared using parameters that describe the dielectric response of the constituents, namely, silica, air and the corresponding metals, assuming that the properties of the constituents remain qualitatively unchanged. This approach would not work for the stop bands in the visible range; however in the mid-IR range it should be correct since $\lambda \gg d$. We write for $\varepsilon(\omega)$

$$\varepsilon = 0.26(1-f)\varepsilon_{\text{air}} + 0.26f\varepsilon_{\text{M}} + 0.74\varepsilon_{\text{Si}}, \quad (1)$$

where ε_{air}, ε_{M} and ε_{Si} are the frequency dependent dielectric functions for air (=1), metal and silica, respectively, and f is the metal filling factor for the voids. The coefficient 0.26 for air and metal and 0.74 for silica are the volume fractions of the balls and voids, respectively, in a typical face-centered-cubic (fcc) type Bravais lattice.

Downloaded 01 Dec 2009 to 155.97.11.183. Redistribution subject to AIP license or copyright; see http://jap.aip.org/jap/copyright.jsp

TABLE I. The best fitting parameters of the dielectric function, $\varepsilon(\omega)$, that describes the reflectivity spectra of opal, pure Bi, pure Ga, and corresponding infiltrated MDPC samples. $\varepsilon(\infty)$ is the dielectric constant at high frequencies; f is the metal filling factor of the opal voids; γ is the bandwidth; S is the oscillator strength; ω_p is the free electron plasma frequency; and ω_T is a resonance frequency for IR activity.

Material	$\varepsilon(\infty)$	f	γ (eV)	S	ω_p (eV)	ω_T (eV)
Silica	2.0	···	0.01	0.45	···	0.14
Bi	12.6	···	1.7	48.8	···	1.20
Ga	···	···	···	···	13.8[a]	···
Bi MDPC	2.7	0.8[a]	0.90	10.0	···	0.46
Ga MDPC	1.0	1.0[a]	16.0	···	13.8[a]	···

[a]These parameters were taken as constants in the fitting program.

First we fit $\varepsilon(\omega)$ of the uninfiltrated opal, $\varepsilon_{\text{opal}}$, to obtain the optical parameters of silica,

$$\varepsilon_{\text{opal}} = 0.26 + 0.74\left(\varepsilon_{\text{Si}}(\infty) + \frac{s_{\text{Si}}\omega_{\text{Si}T}^2}{\omega_{\text{Si}T}^2 - \omega^2 - i\omega\gamma_{\text{Si}}}\right). \quad (2)$$

Here the coefficient 0.26 comes from the voids, $\varepsilon_{\text{Si}}(\infty)$ $(=2.0)$ is the dielectric constant of silica at high frequencies, s_{Si} is the oscillator strength of silica at the ν_2 phonon band, and $\omega_{\text{Si}T}$ (γ_{Si}) is the frequency (width) of the IR active phonon. The least square fitting parameters s_{Si}, $\omega_{\text{Si}T}$ and γ_{Si} are given in Table I, and the $R(\omega)$ spectrum calculated using Eq. (2) based on these parameters is shown in Fig. 1 (dashed line).

A similar procedure was used to fit the dielectric function, ε_{Bi}, of pure Bi; in this case we chose a Lorentzian to fit the resonance ω_{VC} observed at low frequencies:[24]

$$\varepsilon_{\text{Bi}} = \varepsilon_{\text{Bi}}(\infty) + \frac{s_{\text{Bi}}\omega_{\text{Bi}T}^2}{\omega_{\text{Bi}T}^2 - \omega^2 - i\omega\gamma_{\text{Bi}}}. \quad (3)$$

Here $\varepsilon_{\text{Bi}}(\infty)$, s_{Bi}, $\omega_{\text{Bi}T}$ and γ_{Bi} have the same meanings as those mentioned above for the opal. The best fitting parameters are given in Table I and the corresponding $R(\omega)$ spectrum using Eq. (3) with these parameters is shown in Fig. 2(a). Consequently to fit the $R(\omega)$ spectrum in Bi MDPC we used Eq. (1) with the dielectric parameters of Bi and opal determined above. As fitting parameters we left free $\varepsilon_{\text{Bi}}(\infty)$, γ_{Bi} and $\omega_{\text{Bi}T}$. These fitting parameters are given in Table I and the corresponding $R(\omega)$ spectrum is shown in Fig. 2(c). The good agreement with the experimental data validates the model used.

For Ga MDPC the fitting procedure was similar to that of Bi MDPC, except that we used the following Drude model to describe the Ga metallic dielectric function, ε_{Ga}:

$$\varepsilon_{\text{Ga}} = \varepsilon_{\text{Ga}}(\infty) - \frac{\omega_P^2}{\omega^2 + i\omega\gamma_{\text{Ga}}}, \quad (4)$$

where $\varepsilon_{\text{Ga}}(\infty)$ is the contribution from the ion cores, and ω_p and γ_{Ga} are the plasma frequency and collision rate, respectively, of free electrons in gallium. Equation (4) was used for ε_{M} in Eq. (1), with $f=1$ and $\omega_p = 13.8$ eV,[27] and keeping $\varepsilon_{\text{Ga}}(\infty)$ and γ_{Ga} as free parameters. The best fitting parameters are given in Table I and the corresponding reflectivity spectrum, which is in good agreement with the experimental data, is shown in Fig. 3(c). Again the good fit validates the approach taken to describe the dielectric response in the MDPC for wavelengths much larger than the periodicity, $\lambda \gg d$, which cannot be described using Bragg interference.

IV. CONCLUSIONS

In conclusion we fabricated MDPCs by infiltrating metals into opal PCs at high pressure and elevated temperature. The reflectivity spectra show features that are typical of metals but also of uninfiltrated opals. The reflectivity is very low in the visible/NIR spectral range; this allows the penetration of light beyond the metal skin depth, typically a few hundred nm, making it possible to form relatively broad Bragg stop bands in the visible range. However in the mid-IR range below a cut-off frequency ω_c the reflectivity abruptly increases to its normal bulk value in the corresponding metal, giving the impression of a redshifted plasma edge. A model calculation, in which the MDPC dielectric response is composed of the dielectric response of the constituents describes well the reflectivity spectrum for $\lambda \gg d$, that is away from the Bragg stop bands.

ACKNOWLEDGMENTS

The authors acknowledge useful discussions with Dr. Efros and Dr. Pokrovsky, and help from Dr. Wohlgenannt and Dr. Jiang with the optical measurements. Financial support from the NSF–NIRT program, Grant No. DMR-0102964, and ARO Grant No. DAAD 19-03-1-0290 are gratefully acknowledged. One of the authors (V.K.) also acknowledges support from the PRF, administrated by the ACS, under Grant No. 36802-ACS.

[1] E. R. Brown and O. B. McMahon, Appl. Phys. Lett. **67**, 2138 (1995).
[2] S. Gupta, G. Tuttle, M. Sigalas, and K. M. Ho, Appl. Phys. Lett. **71**, 2412 (1997).
[3] M. Scalora, M. J. Bloemer, A. S. Pethel, J. P. Dowling, C. M. Bowden, and A. S. Manka, J. Appl. Phys. **83**, 2377 (1998).
[4] A. Sievenpiper, M. E. Sickmiller, E. Yablonovitch, J. N. Winn, S. Fan, P. R. Villenneuve, and J. D. Joannopoulos, Phys. Rev. Lett. **80**, 2829 (1998).
[5] O. D. Velev, P. M. Tessier, A. M. Lenhoff, and E. W. Kaler, Nature (London) **401**, 548 (1999).
[6] J. E. G. J. Wijnhoven, S. J. M. Zevenhuizen, M. A. Hendriks, D. Vanmaekelbergh, J. J. Kelly, and W. L. Vos, Adv. Mater. (Weinheim, Ger.) **12**, 888 (2000).
[7] G. L. Egan, J.-S. Yu, C. H. Kim, S. J. Lee, R. E. Schaak, and T. E. Mallouk, Adv. Mater. (Weinheim, Ger.) **12**, 1040 (2000).
[8] J. Zhou, Y. Zhou, S. L. Ng, H. X. Zhang, W. X. Que, Y. L. Lam, Y. C. Chan, and C. H. Kam, Appl. Phys. Lett. **76**, 3337 (2000).
[9] K. M. Kulinowski, P. Jiang, H. Vaswani, and V. L. Colvin, Adv. Mater. (Weinheim, Ger.) **12**, 833 (2000).
[10] A. A. Zakhidov, R. H. Baughman, I. I. Khayrullin, I. Udod, M. Kozlov, N. Eradat, Z. V. Vardeny, M. Soukolis and R. Biswas, Synth. Met. **116**, 419 (2001).
[11] Z. Liang, A. S. Susha, F. Caruso, Adv. Mater. (Weinheim, Ger.) **14**, 1160 (2002).
[12] J. G. Fleming, S. Y. Lin, I. El-Kady, R. Biswas, and K. M. Ho, Nature (London) **417**, 52 (2002).
[13] S.-Y. Lin, J. G. Fleming, and I. El-Kady, Appl. Phys. Lett. **83**, 593 (2003).
[14] A. A. Maradudin and A. R. McGurn, Phys. Rev. B **48**, 17576 (1993).
[15] M. M. Sigalas, C. T. Chan, K. M. Ho, and C. M. Soukoulis, Phys. Rev. B **52**, 11744 (1995).
[16] J. B. Pendry, A. J. Holden, W. J. Stewart, and I. Youngs, Phys. Rev. Lett. **76**, 4773 (1996).
[17] A. Moroz, Phys. Rev. Lett. **83**, 5274 (1999).
[18] A. K. Sarychev and V. M. Shalaev, Phys. Rep. **335**, 275 (2000).

Downloaded 01 Dec 2009 to 155.97.11.183. Redistribution subject to AIP license or copyright; see http://jap.aip.org/jap/copyright.jsp

[19] A. L. Pokrovsky and A. L. Efros, Phys. Rev. B **65**, 045110 (2002).
[20] A. L. Pokrovsky and A. L. Efros, Phys. Rev. Lett. **89**, 093901 (2002).
[21] A. A. Zakhidov, R. H. Baughman, Z. Iqbal, C. Cui, I. Khayrullin, S. O. Dantas, J. Marti, and V. G. Ralchenko, Science **282**, 897 (1998).
[22] V. F. Kozhevnikov, M. Diwekar, V. P. Kamaev, J. Shi, and Z. V. Vardeny, Physica B **338**, 159 (2003).
[23] J. R. Martinez *et al.*, J. Chem. Phys. **109**, 7511 (1998).
[24] M. Cardona and D. L. Greenaway, Phys. Rev. **133**, A1685 (1964).
[25] E. Gerlach, P. Grosse, M. Rautenberg, and W. Senske, Phys. Status Solidi B **75**, 553 (1976).
[26] L. M. Glaessen, A. G. Jansen, and P. Wyder, Phys. Rev. B **33**, 7947 (1986).
[27] I. N. Shklyareskii, Y. Y. Bondarenko, and N. A. Makarovskii, Opt. Spectrosc. **88**, 547 (2000).

Downloaded 01 Dec 2009 to 155.97.11.183. Redistribution subject to AIP license or copyright; see http://jap.aip.org/jap/copyright.jsp